nature neuroscience

GABA progenitors grafted into the adult epileptic brain control seizures and abnormal behavior

Robert F Hunt[1,2], Kelly M Girskis[1,2], John L Rubenstein[3], Arturo Alvarez-Buylla[2] & Scott C Baraban[1,2]

Impaired GABA-mediated neurotransmission has been implicated in many neurologic diseases, including epilepsy, intellectual disability and psychiatric disorders. We found that inhibitory neuron transplantation into the hippocampus of adult mice with confirmed epilepsy at the time of grafting markedly reduced the occurrence of electrographic seizures and restored behavioral deficits in spatial learning, hyperactivity and the aggressive response to handling. In the recipient brain, GABA progenitors migrated up to 1,500 μm from the injection site, expressed genes and proteins characteristic for interneurons, differentiated into functional inhibitory neurons and received excitatory synaptic input. In contrast with hippocampus, cell grafts into basolateral amygdala rescued the hyperactivity deficit, but did not alter seizure activity or other abnormal behaviors. Our results highlight a critical role for interneurons in epilepsy and suggest that interneuron cell transplantation is a powerful approach to halting seizures and rescuing accompanying deficits in severely epileptic mice.

GABA-producing inhibitory interneurons are essential for regulating cortical excitability and coordinating appropriate behaviors. In hippocampus, interneuron dysfunction has been implicated in many forms of epilepsy[1,2] and can disrupt learning and memory[3] or social behaviors[4]. Current medications that systemically potentiate GABA-mediated inhibition can be effective at suppressing seizures, but prolonged drug treatment can have unwanted cognitive or neurobehavioral side effects and epilepsy remains refractory to medical treatment in nearly one-third of affected individuals[5]. Recently, optogenetic techniques have been used to interrupt seizure activity in animal models of epilepsy[6,7], supporting the general concept that focal inhibition of epileptic networks might have therapeutic application. Although promising, these approaches require expression of light-sensitive opsins, invasive light delivery interface and seizure-detection hardware. Transplantation and subsequent integration of new inhibitory neurons into neural circuits affected by epilepsy might be a therapeutic strategy for controlling seizures, or other co-occurring behaviors, as a one-time procedure without the need for regular neural modulation or online seizure prediction.

The majority of cortical interneurons are born in the medial ganglionic eminence (MGE) of the embryonic ventral telencephalon[8–11]. When grafted into the neonatal brain, MGE progenitor cells migrate long distances and functionally integrate as inhibitory neurons[9,12–14]. Previously, we found that early postnatal transplantation of GABA progenitor cells into neocortex, before seizure onset, reduced spontaneous electrographic seizure activity in mice with a congenital potassium channel mutation[13]. However, whether this approach would be successful in the more common and medically refractory types of epilepsy seen in adults has not been directly tested. The emergence of epilepsy in adulthood involves a wide range of modifications to brain structure and function[1,2], and it is not known whether the adult nervous system can support GABA progenitor cell migration, differentiation, integration or functional recovery of pre-existing deficits.

On this basis, we first carefully characterized the development of MGE progenitors grafted into adult recipients. We then asked whether epileptic phenotypes could be improved by MGE cell grafts into the hippocampus or amygdala after epileptic seizures emerge (**Supplementary Fig. 1**). For this purpose, we selected a pilocarpine model of epilepsy that is characterized by robust, frequent spontaneous seizures acquired after a brain insult[15–18], well-described behavioral abnormalities[18] and poor responses to antiepileptic drugs[19]. These animals recapitulate several key features of human temporal lobe epilepsy, the most common type of epilepsy in adults[1,2].

RESULTS

We obtained MGE progenitors from embryonic day 13.5 (E13.5) *GFP*$^+$ donor mice[20], in which the EGFP gene is driven by a CMV (cytomegalovirus) immediate early enhancer coupled to the chicken β-actin (*ACTB*) promoter, as described previously[9,12–14], and injected 3×10^4 cells into the dorsal hippocampus of adult (postnatal day 60, P60) control recipients. The migration (**Fig. 1a**) and neurochemical expression (**Fig. 1b**) of grafted cells was examined 7 and 60 d after transplantation (DAT). By 7 DAT, GFP$^+$ MGE cells had moved away from the injection and dispersed throughout hippocampal subfields ($n = 3$ mice; **Supplementary Fig. 2**). Many grafted cells were found along major fiber tracts and exhibited a bipolar, migratory morphology, whereas others started to extend multiple processes from the cell body. Survival rate at 7 DAT was 32.6 ± 2.3% ($n = 3$). By 60 DAT ($n = 6$ mice), these cells had migrated up to 1,500 μm from the injection site, and cell survival was 14.8 ± 1.3%. We did not detect a significant

[1]Epilepsy Research Laboratory, University of California, San Francisco, California, USA. [2]Department of Neurological Surgery, University of California, San Francisco, California, USA. [3]Department of Psychiatry, University of California, San Francisco, California, USA. Correspondence should be addressed to R.F.H. (robert.huntiii@ucsf.edu) or S.C.B. (scott.baraban@ucsf.edu).

Received 6 December 2012; accepted 26 March 2013; published online 5 May 2013; doi:10.1038/nn.3392

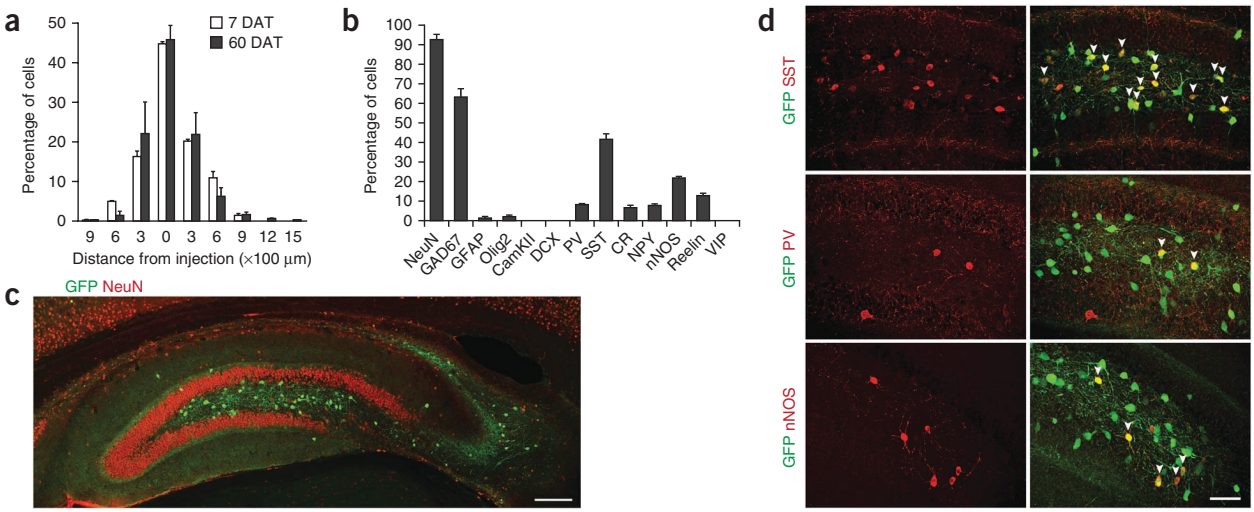

Figure 1 Transplanted MGE cells migrate into the adult hippocampus and express markers of inhibitory neurons. (**a**) Distribution of transplanted E13.5 MGE cells expressing GFP 7 DAT (white bars, $n = 3$ mice) and 60 DAT (gray bars, $n = 6$ mice). (**b**) Quantification of marker expression in GFP-labeled cells ($n = 3$–6 mice per marker). CR, calretinin; GFAP, glial fibrillary acid protein; DCX, doublecortin; nNOS, neuronal nitric oxide synthase; NPY, neuropeptide Y; PV, parvalbumin; SST, somatostatin; VIP, vasoactive intestinal peptide. (**c**) Hippocampus of a pilocarpine-injected recipient mouse (60 DAT) labeled for NeuN (red) and transplanted GFP-labeled inhibitory neurons (green). Transplanted neurons dispersed after grafting into recipient mice despite extensive hippocampal cell loss resulting from pilocarpine injection. (**d**) At 60 DAT, GFP-labeled cells (green) coexpressed somatostatin, parvalbumin and neuronal nitric oxide synthase (all in red). Arrowheads, colabeled cells; error bars, s.e.m.; scale bars, 1,000 µm (**c**) and 67 µm (**d**).

difference between the mean rostrocaudal distance of grafted MGE cells at 60 DAT and that at 7 DAT ($P = 0.44$, two-tailed t-test; **Fig. 1a**), suggesting that rostrocaudal migration is nearly complete by 7 DAT. At 60 DAT, most GFP-labeled cells exhibited the morphological features of mature interneurons, with large, extensive processes and cell bodies positioned in regions normally occupied by endogenous inhibitory neurons (that is, polymorph and molecular layers). GFP-labeled cells expressed NeuN (92.2 ± 2.9%), GAD67 (63 ± 4.4%) and interneuron markers, with somatostatin (41.3 ± 2.8%), neuronal nitric oxide synthase (21.6 ± 1.2%) and parvalbumin (7.7 ± 0.8%)

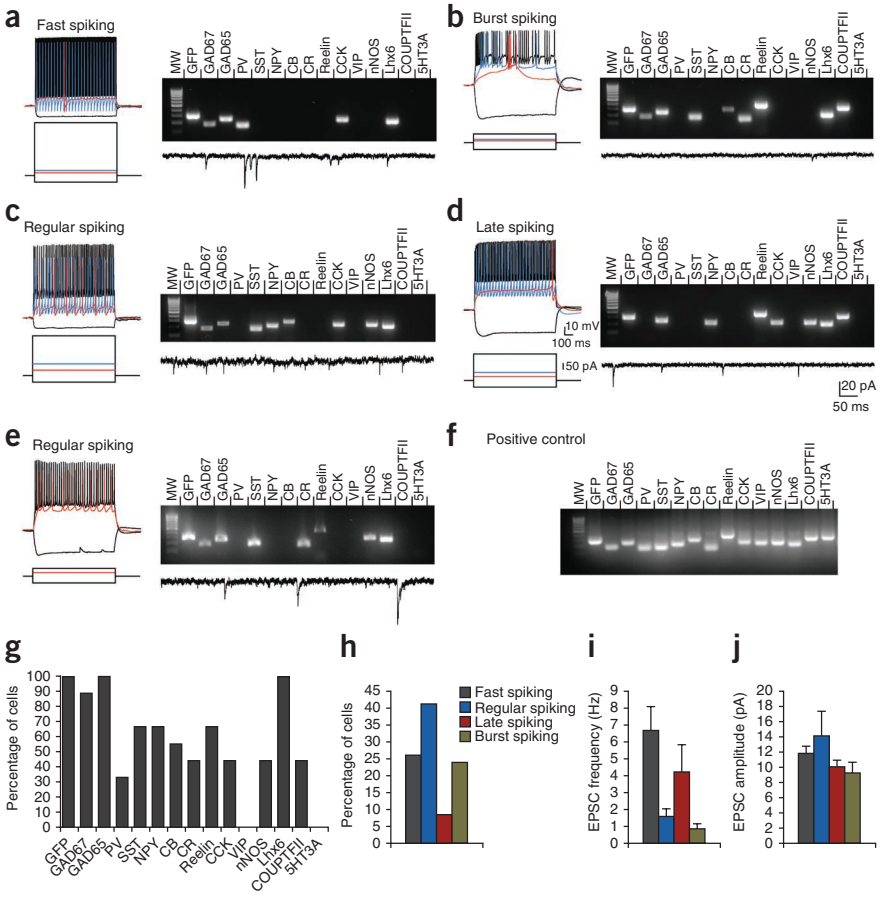

Figure 2 Transplanted MGE cells differentiate into functional inhibitory interneurons. (**a**–**e**) Example electrophysiological responses of five different transplanted MGE cells to the indicated square wave current pulses (bottom) from a holding potential near –70 mV. Recordings were obtained from slices 61–65 DAT. Depolarizing current pulses and corresponding responses are for near threshold (red), 2× threshold (blue) and near maximal firing (black). Right, RNA profiles obtained from single-cell RT-PCR analysis for each recorded cell. MW, molecular weight marker; CB, calbindin; CCK, cholecystokinin. (**f**) Positive control for the single-cell RT-PCR procedure using 1 ng of hippocampus RNA from a GFP$^+$ mouse. (**g**) Summary plot for the occurrence of each marker in recorded GFP$^+$ cells ($n = 9$ cells). RNA was obtained from regular-spiking ($n = 3$), fast-spiking ($n = 2$), burst-spiking ($n = 3$) and late-spiking ($n = 1$) interneurons. (**h**) Occurrence of each interneuron subtype recorded based on firing properties ($n = 46$ cells). (**i**,**j**) Mean EPSC frequency (**i**) and amplitude (**j**) according to interneuron subtype. Error bars represent s.e.m. Electrophysiological properties of grafted interneurons are summarized in **Supplementary Table 2**.

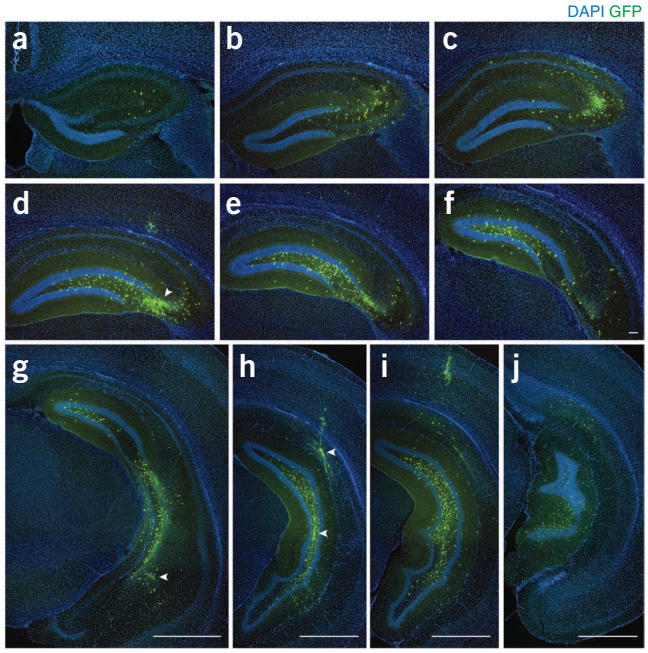

Figure 3 Distribution of MGE-derived cells 60+ DAT into the adult epileptic hippocampus. (**a**–**j**) Serial sections (300 µm apart) through the entire hippocampus of a pilocarpine-treated recipient mouse labeled for transplanted MGE cells (green) and DAPI (blue). Arrowheads in **d**,**g**,**h** indicate injection sites. Scale bars, 100 µm (**a**–**f**) and 1,000 µm (**g**–**j**).

subtypes representing the majority of colabeled cells, as reported previously[8–10]. We also examined other GABAergic subtypes, including those expressing calretinin (6.4 ± 1.3%), neuropeptide Y (7.5 ± 1.1%), reelin (12.5 ± 1.5%) and vasoactive intestinal peptide (0%). None of the GFP$^+$ MGE cells expressed CamKII (excitatory neurons) or doublecortin (immature neurons). A small percentage of cells around the injection site colabeled for olig2 (oligodendrocytes, 1.8%) or glial fibrillary acid protein (astrocytes, 1%) and failed to exhibit neuronal electrophysiological properties (**Supplementary Fig. 3**). We obtained similar results using adult epileptic mice as recipients, indicating that dispersion or marker expression of the transplanted cells were not affected in epileptic mice (**Fig. 1c**,**d**).

Next, we examined the electrophysiological and molecular properties of GFP$^+$ MGE neurons using visualized patch-clamp recordings in combination with *post hoc* single-cell reverse transcription (RT)-PCR. In acute hippocampal slices from transplanted mice (60–65 DAT), GFP$^+$ MGE cells exhibited electrophysiological phenotypes and RNA expression profiles consistent with those of mature interneurons of a MGE lineage[21] (**Fig. 2** and **Supplementary Table 1**). Electrophysiological recordings from 46 cells revealed four main subtypes of interneurons: fast spiking (n = 12 cells, 26%), regular spiking nonpyramidal (n = 19 cells, 41%), late spiking (n = 4 cells, 9%) and burst spiking (n = 11 cells, 24%). All interneurons examined by single-cell RT-PCR (n = 9 interneurons) expressed *Lhx6*, a transcription factor expressed in MGE-derived interneurons, and other gene markers expressed in MGE-derived GABA neurons (**Fig. 2a**–**g**). None of the recorded cells contained RNA for the ionotropic serotonin receptor 5HT3A or vasoactive intestinal peptide, which are expressed in cortical interneurons from the caudal ganglionic eminence[21]. Voltage-clamp recordings confirmed the presence of spontaneous excitatory postsynaptic currents in all of the grafted interneurons (**Fig. 2i**,**j** and **Supplementary Table 2**), consistent with functional integration of these cells into the hippocampal network. Taken together, these findings indicate that the adult hippocampus is permissive for migration and functional integration of embryonic GABA progenitors and that these cells differentiate into mature interneurons.

To test the effect of transplanted MGE cells on spontaneous seizures, we performed continuous video-electroencephalographic (video-EEG) monitoring in the pilocarpine model[18,19]. After an acute episode of pilocarpine-induced status epilepticus, P51 adult mice were first video monitored for 9–20 d to document the emergence of at least one spontaneous seizure before random assignment into untreated, vehicle-injected or MGE cell–injected groups (**Supplementary Fig. 1**). After seizure confirmation, we made bilateral injections of MGE cells into hippocampus (four injections of 3 × 10^4 cells per hippocampi). This approach distributed newly generated inhibitory neurons throughout the adult hippocampus of epileptic recipients at 60+ DAT (**Fig. 3**). In a separate group of mice, we made bilateral injections into the basolateral amygdala (a single injection of 3 × 10^4 cells per hemisphere); dispersion and marker expression of MGE cell grafts into the amygdala were comparable to hippocampus (**Fig. 4**). We chose these brain regions because they exhibit substantial neuropathology[1,2,15,22], including inhibitory neuron loss, and contribute to seizure generation in this model[1,2,17].

All of the untreated (n = 7 mice) or vehicle-injected (n = 7) epileptic mice displayed spontaneous electrographic seizures (**Fig. 5a**), consisting of high-frequency, high-voltage, rhythmic activity with clear onset and termination and prominent voltage spikes preceding ictal events (frequency = 2.36 ± 0.46 seizures per day, n = 14 mice). Electrographic seizures or high-voltage spiking were never observed in naive control mice that did not receive pilocarpine (n = 3 mice). Simultaneous video monitoring confirmed convulsive, Racine stage 3–5 seizure behaviors during electrographic events[23] (**Supplementary Movie 1**). Epileptic mice that received injections of MGE cells into the hippocampus exhibited a 92% reduction in seizure frequency (frequency = 0.17 ± 0.09, n = 8 mice; **Fig. 5b**). In 50% of these mice, no electrographic seizures were observed during the entire video-EEG monitoring period (7–10 d). In contrast, transplantation into the basolateral amygdala had no effect on seizure frequency (frequency = 2.24 ± 0.46, n = 8 mice). The duration of electrographic events or behavioral severity was not different in MGE-grafted mice than in untreated or vehicle-injected epileptic mice (**Supplementary Table 3**).

We next asked whether MGE cell transplantation affected mossy fiber sprouting into the inner molecular layer of the dentate gyrus, a well-characterized pathology in epilepsy patients and animal models[1,2,15,24]. To visualize mossy fibers, we stained for zinc transporter 3 (ZnT3), which is highly expressed in mossy fiber terminals[25] (**Supplementary Fig. 4**), and assigned Timm scores from 0 (little to no sprouting) to 3 (robust sprouting), as previously described[15]. Robust mossy fiber sprouting was present in all vehicle-injected epileptic mice (Timm score = 2.85 ± 0.1, n = 4 mice) and at 60 DAT in mice that received MGE cell grafts into the hippocampus (Timm score = 2.75 ± 0.13, n = 4 mice), but not in controls (Timm score = 0, n = 4 mice). One-way ANOVA on ranks analysis revealed that Timm scores for mossy fiber sprouting were not significantly different between vehicle-injected epileptic mice and those that received MGE cell grafts (H = 8.045, Tukey's *post hoc*, $P > 0.05$), but both groups had significantly greater Timm scores than controls ($P < 0.05$). This observation suggests that the marked decrease in seizures obtained with MGE cell transplantation was not a result of a reversal of abnormal mossy fiber sprouting in the dentate gyrus.

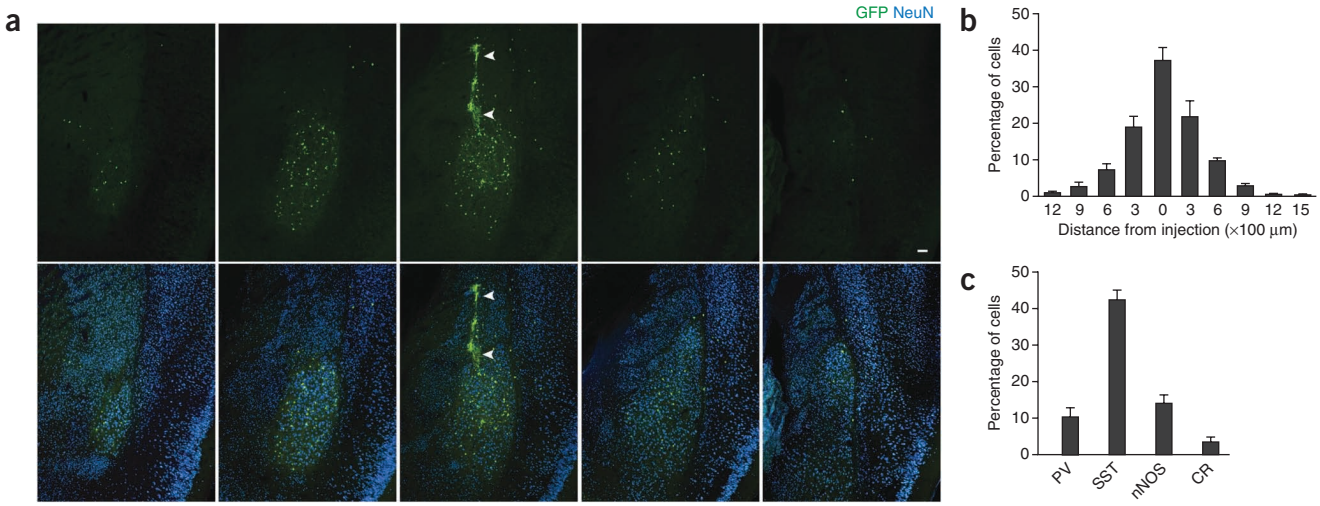

Figure 4 Distribution of MGE-derived cells 60+ DAT into the adult epileptic amygdala. (**a**) Serial sections (300 μm apart) through the amygdala of a pilocarpine-treated recipient mouse labeled for transplanted MGE cells (green) and NeuN (blue). Cells were distributed throughout the lateral and basal nuclei, but were rarely found lateral to the external capsule. Arrowheads indicate injection tract. Scale bar, 100 μm. (**b**) Distribution of transplanted E13.5 MGE cells 60 DAT ($n = 6$ mice). (**c**) Quantification of marker expression in GFP-labeled cells ($n = 3$ mice per marker). Error bars, s.e.m.

Quality of life in epilepsy patients is often markedly affected by cognitive decline, and epilepsy can be accompanied by debilitating neurobehavioral comorbidities, including psychiatric disorders, anxiety or social problems[26]. Thus, we examined whether MGE cell transplantation could rescue any of the well-characterized behavioral phenotypes associated with the pilocarpine model[18]. A handling test revealed that epileptic mice had a marked increase in their reaction to handling. All of the epileptic mice displayed aggressive behaviors to touch, which were rare in controls. MGE cell transplantation into hippocampus rescued this abnormal behavior to control levels, but transplantation into amygdala had no effect (**Fig. 6a** and **Supplementary Movie 2**). During a 10-min open field test (locomotion), epileptic mice displayed hyperactivity and traveled significantly farther than controls ($P < 0.01$). This behavioral deficit was reversed by cell transplantation into the hippocampus or amygdala (**Fig. 6b**). In an accelerating rotarod assay (motor coordination), we did not observe a significant difference among treatment groups in either the r.p.m. reached ($P = 0.31$) or the amount of time spent on the rod ($P = 0.38$; **Fig. 6c**,**d**). In the elevated plus maze (general anxiety), we did not observe differences among treatment groups in either the number of open arm entries ($P = 0.16$) or the amount of time spent in the open arms ($P = 0.12$; **Fig. 6e**,**f**). In the forced swim test (despair), control mice developed a characteristic immobile posture when placed into a water-filled cylinder from which they could not escape, but most epileptic mice continued to swim, trying to escape the cylinder throughout the test duration. MGE transplantation into the hippocampus or amygdala of epileptic mice did not alter this behavior (**Fig. 6g**).

Finally, we asked whether MGE cell transplantation affected performance in a Morris water maze test, which requires the use of external visual cues to locate a hidden platform and escape the water. We first examined the mice's ability to locate a visible platform (cued learning) and to then locate a hidden platform (acquisition). Next, we removed the hidden platform (probe trial) to measure the short-term retention of spatial memory. Nearly all of the mice showed improvement in the time to find the visible platform, demonstrating efficient cued learning (**Fig. 6h**); two mice in the 'epilepsy' group and one mouse that received MGE cell grafts into amygdala were excluded from further analysis because they showed a substantial deficit in the visible platform training (**Supplementary Fig. 5**), which can confound the interpretation of spatial learning deficits in the hidden platform task[27,28]. During the hidden platform test (**Fig. 6i**), epileptic mice that did not receive MGE cell grafts had significantly longer escape latencies than controls ($P < 0.001$), consistent with previous reports and impaired spatial learning[18,27,28], although the possibility that noncognitive deficits might influence water maze performance in these mice cannot be excluded. This deficit was confirmed in a probe test 1 h after the final testing session (**Fig. 6j–l**). Although control mice spent significantly more time in the target quadrant ($P < 0.001$) and made numerous platform crossings, epileptic mice showed no preference for any quadrant ($P = 0.4$) and rarely crossed the platform location. MGE cell transplantation into hippocampus rescued these deficits in escape latencies, quadrant time and platform crossings to control levels. However, mice that received MGE cell grafts into

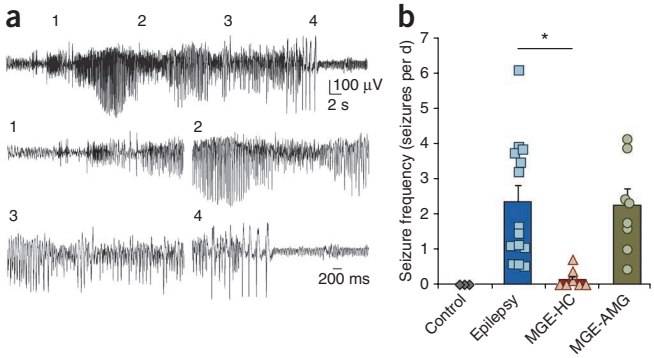

Figure 5 Inhibitory neuron transplantation reduces seizure occurrence in epileptic mice. (**a**) Example EEG recording of a spontaneous seizure from an untreated epileptic mouse. Numbers indicate the regions of the seizure shown below at high resolution. (**b**) Bar plots show the mean spontaneous seizure frequency (seizures per d) for each group based on continuous EEG recordings (7–10 d). Bars represent mean ± s.e.m. The data points superimposed over the bar graph each represent an individual mouse from which recordings were obtained. $^*P < 0.01$. MGE-HC, MGE transplantation into the hippocampus; MGE-AMG, MGE transplantation into the amygdala.

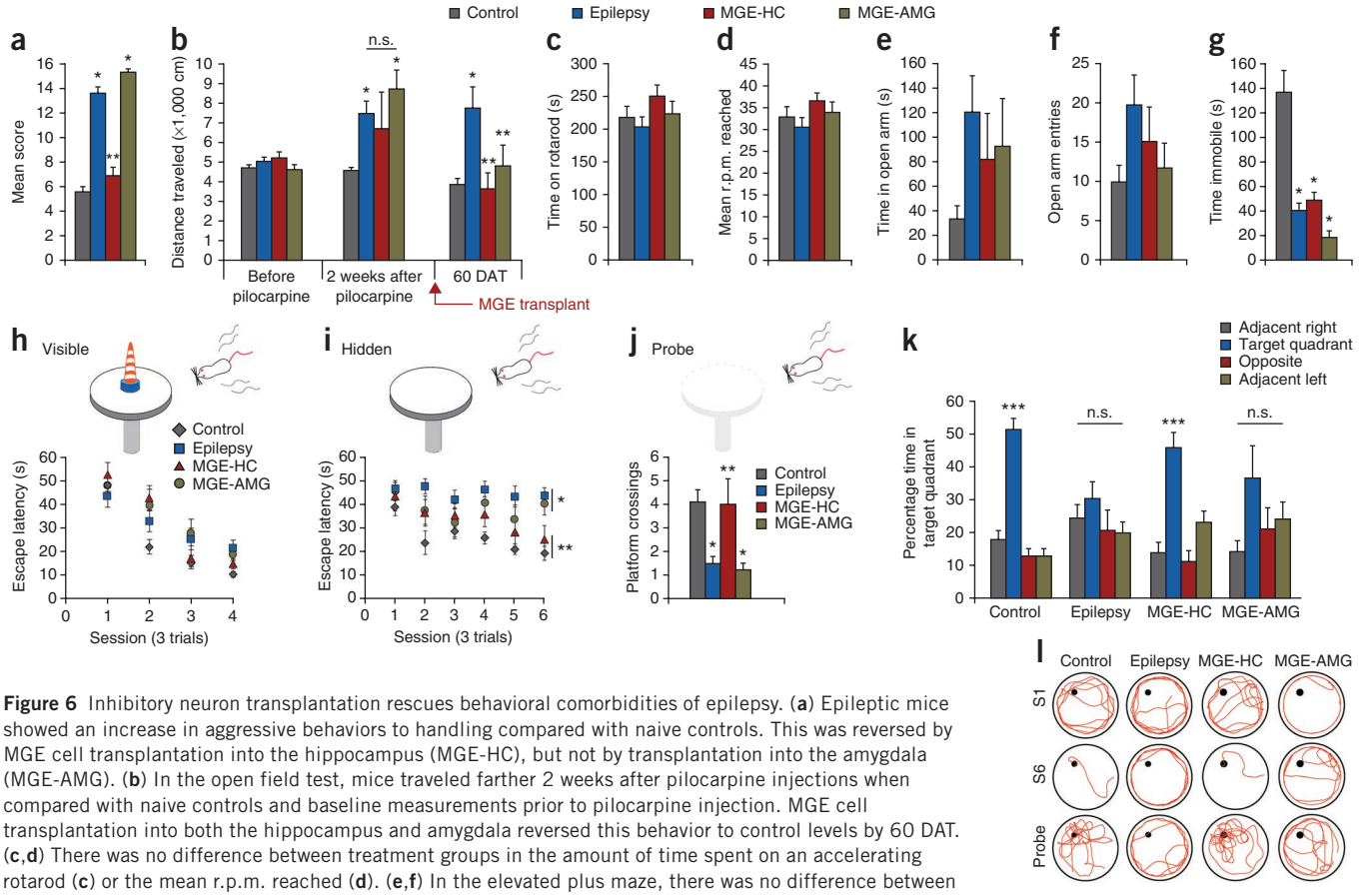

Figure 6 Inhibitory neuron transplantation rescues behavioral comorbidities of epilepsy. (**a**) Epileptic mice showed an increase in aggressive behaviors to handling compared with naive controls. This was reversed by MGE cell transplantation into the hippocampus (MGE-HC), but not by transplantation into the amygdala (MGE-AMG). (**b**) In the open field test, mice traveled farther 2 weeks after pilocarpine injections when compared with naive controls and baseline measurements prior to pilocarpine injection. MGE cell transplantation into both the hippocampus and amygdala reversed this behavior to control levels by 60 DAT. (**c**,**d**) There was no difference between treatment groups in the amount of time spent on an accelerating rotarod (**c**) or the mean r.p.m. reached (**d**). (**e**,**f**) In the elevated plus maze, there was no difference between treatment groups in the amount of time spent in the open arm (**e**) or the number of open arm entries (**f**). (**g**) In the forced swim test, epileptic mice spent less time immobile than control mice, and MGE transplantation into the hippocampus or amygdala did not improve this behavior. (**h**) In a Morris water maze test, all mice showed a decrease in latency to escape the maze during repeated training trials in the visible platform test. (**i**) Epileptic mice showed a marked deficit in latency to escape the maze during the six repeated sessions of the hidden platform test. (**j**,**k**) During a probe trial following the final testing session, epileptic mice made fewer platform crossings (**j**) and did not show a preference for any quadrant (**k**). MGE cell transplantation into hippocampus, but not transplantation into amygdala, rescued deficits in escape latency (**i**) and probe trial performance (**j**,**k**) with control levels. (**l**) Example locomotion tracking plots showing the total path-length during session 1 (S1) and session 6 (S6) of the hidden platform task and the probe trial. Black circle indicates platform location. All data represent mean ± s.e.m. from 6–25 mice per treatment group. $*P < 0.05$ versus control, $**P < 0.05$ versus epilepsy, $***P < 0.001$ versus other quadrants; n.s., not significant ($P = 0.4$ for epilepsy group and $P = 0.11$ for MGE-AMG group). All values and statistical analyses are provided in **Supplementary Table 3**.

amygdala did not show improvement in spatial learning and were indistinguishable from untreated epileptic mice.

DISCUSSION

We found that MGE progenitor cells grafted into the adult epileptic brain exerted a substantial therapeutic effect on seizures and abnormal behaviors commonly associated with epilepsy. The degree to which this procedure was successful in abrogating seizures in the pilocarpine model was notable given that neuropathology (for example, mossy fiber sprouting) as a result of pre-existing limbic epilepsy remained present in these mice and the reported difficulty of controlling spontaneous seizures using conventional antiepileptic treatments[19]. Improved behavior after MGE cell grafting into epileptic mice could be relevant to other brain disorders that involve a disruption of inhibitory circuits in hippocampus, such as Alzheimer's disease[29] or autism[4]. Not surprisingly, these neurological disorders often involve increased seizure susceptibility as a co-morbidity. Interneuron-based cell transplantation might have an important clinical advantage over current therapeutic approaches in that cell grafts can be targeted to spatially restricted brain regions as a one-time procedure for seizure control. In addition to the obvious benefits for promoting functional recovery, this approach might also be useful for limiting adverse behavioral side effects that can be associated with medications or for sparing areas of the epileptic brain normally targeted for surgical resection.

Although our goal was not to examine the site of seizure initiation in this epilepsy model, we did find that interneuron cell grafts into the hippocampus, but not the amygdala, were critical for controlling epileptic activity. Despite the potentially widespread tissue damage associated with systemic pilocarpine administration[1,2,12,19], these findings are consistent with reports that around 70% of electrographic seizure events involve the hippocampal formation in this model[17]. Our findings support a critical role for the loss of inhibitory neurons in epilepsy, a pathology that likely contributes to the reduced synaptic inhibition observed in the hippocampus of epileptic pilocarpine-treated rodents[30–32]. Enhancement of GABA-mediated synaptic inhibition that is associated with new MGE-derived interneurons[12–14,33] further supports the concept that abnormal electrical activity is kept in check by a powerful interneuron-mediated 'inhibitory restraint'[34–36] and that this enhancement may be sufficient to prevent seizure initiation. Given that we assessed mice around 80–100 d after the induction of

status epilepticus, a time at which epilepsy is well established in this model, it also seems reasonable to conclude that GABA progenitor cell transplantation has long-term effects on seizures and behavior.

A major challenge in the field has been to develop new approaches for controlling epilepsies that do not respond to current medications. Our results suggest that GABA progenitors are particularly promising candidates for cell therapy, as they can be broadly distributed in spatially restricted brain regions in adult behaving mice. This approach is based on the functional engraftment of new inhibitory interneurons into existing circuits and, in contrast with optogenetics-based[6,7] or stimulation-based[37] approaches, does not require a system for real-time seizure detection. Although production of a comparable and safe MGE-like human stem cell line will ultimately be necessary before translation to the clinic, our results are an encouraging step toward using inhibitory neurons for brain repair in adults with severe forms of epilepsy.

METHODS

Methods and any associated references are available in the online version of the paper.

Note: Supplementary information is available in the online version of the paper.

ACKNOWLEDGMENTS

We thank M. Dinday and W. Hindle-Katel for assistance with pilocarpine injections, J. Sebe for tissue dissection training, G. Hortopan for advice on the single-cell RT-PCR procedure, R. Palmiter for the ZnT3 antibody, and S. Canchola for training on behavior assays. This work was supported by funding from US National Institutes of Health grants from the National Institute of Neurological Disorders and Stroke (RO1-NS071785 to S.C.B., J.L.R. and A.A.-B., and F32-NS077747 to R.F.H.), and a grant from the California Institute of Regenerative Medicine (#TR2-01749 to A.A.-B. and S.C.B.).

AUTHOR CONTRIBUTIONS

R.F.H. contributed to the concept, design, execution and analysis of all of the experiments, provided funding, and wrote the manuscript. K.M.G. contributed to the execution and analysis of the immunostaining and behavior experiments. J.L.R. and A.A.-B. contributed to the concept, provided funding and edited the manuscript. S.C.B. contributed to the concept and design of the experiments, analyzed the EEG data, provided funding, and wrote the manuscript.

COMPETING FINANCIAL INTERESTS

The authors declare competing financial interests: details are available in the online version of the paper.

1. Lothman, E.W., Bertram, E.H. III & Stringer, J.L. Functional anatomy of hippocampal seizures. *Prog. Neurobiol.* **37**, 1–82 (1991).
2. Noebels, J.L., Avoli, M., Rogawski, M.A., Olsen, R.W. & Delgado-Escueta, A.V. *Jasper's Basic Mechanisms of the Epilepsies*, 4th edn. (National Center for Biotechnology, Bethesda, Maryland, 2012).
3. Andrews-Zwilling, Y. *et al.* Hilar GABAergic interneuron activity controls spatial learning and memory retrieval. *PLoS ONE* **7**, e40555 (2012).
4. Han, S. *et al.* Autistic-like behavior in *Scn1a*$^{+/-}$ mice and rescue by enhanced GABA-mediated neurotransmission. *Nature* **489**, 385–390 (2012).
5. Anonymous. Epilepsy Fact Sheet. *World Health Organization* ⟨http://www.who.int/mediacentre/factsheets/fs999/en/index.html⟩ (October 2012).
6. Paz, J.T. *et al.* Closed-loop optogenetic control of thalamus as a tool for interrupting seizures after cortical injury. *Nat. Neurosci.* **16**, 64–70 (2013).
7. Krook-Magnuson, E., Armstrong, C., Oijala, M. & Soltesz, I. On-demand optogenetic control of spontaneous seizures in temporal lobe epilepsy. *Nat. Commun.* **4**, 1376 (2013).
8. Lavdas, A.A., Grigoriou, M., Pachnis, V. & Parnavelas, J.G. The medial ganglionic eminence gives rise to a population of early neurons in the developing cerebral cortex. *J. Neurosci.* **19**, 7881–7888 (1999).
9. Wichterle, H., Garcia-Verdugo, J.M., Herrera, D.G. & Alvarez-Buylla, A. Young neurons from medial ganglionic eminence disperse in adult and embryonic brain. *Nat. Neurosci.* **2**, 461–466 (1999).
10. Xu, Q., Cobos, I., De La Cruz, E., Rubenstein, J.L. & Anderson, S.A. Origins of cortical interneuron subtypes. *J. Neurosci.* **24**, 2612–2622 (2004).
11. Butt, S.J. *et al.* The temporal and spatial origins of cortical interneurons predict their physiological subtype. *Neuron* **48**, 591–604 (2005).
12. Alvarez-Dolado, M. *et al.* Cortical inhibition modified by embryonic neural precursors grafted into the postnatal brain. *J. Neurosci.* **26**, 7380–7389 (2006).
13. Baraban, S.C. *et al.* Reduction of seizures by transplantation of cortical GABAergic interneuron precursors into Kv1.1 mutant mice. *Proc. Natl. Acad. Sci. USA* **106**, 15472–15477 (2009).
14. Southwell, D.G. *et al.* Intrinsically determined cell death of developing cortical interneurons. *Nature* **491**, 109–113 (2012).
15. Shibley, H. & Smith, B.N. Pilocarpine-induced status epilepticus results in mossy fiber sprouting and spontaneous seizures in C57BL/6 and CD-1 mice. *Epilepsy Res.* **49**, 109–120 (2002).
16. Goffin, K., Nissinen, J., Van Laere, K. & Pitkänen, A. Cyclicity of spontaneous recurrent seizures in pilocarpine model of temporal lobe epilepsy in rat. *Exp. Neurol.* **205**, 501–505 (2007).
17. Bortel, A., Lévesque, M., Biagini, G., Gotman, J. & Avoli, M. Convulsive status epilepticus duration as determinant for epileptogenesis and interictal discharge generation in the rat limbic system. *Neurobiol. Dis.* **40**, 478–489 (2010).
18. Gröticke, I., Hoffmann, K. & Löscher, W. Behavioral alterations in the pilocarpine model of temporal lobe epilepsy in mice. *Exp. Neurol.* **207**, 329–349 (2007).
19. Löscher, W. Strategies for antiepileptogenesis: antiepileptic drugs versus novel approaches evaluated in post-status epilepticus models of temporal lobe epilepsy. in *Jasper's Basic Mechanisms of the Epilepsies*, 4th edn. (eds. Noebels, J.L., Avoli, M., Rogawski, M.A., Olsen, R.W. & Delgado-Escueta, A.V.) (National Center for Biotechnology Information, Bethesda, Maryland, 2012).
20. Hadjantonakis, A., Gertenstein, M., Ikawa, M., Okabe, M. & Nagy, A. Generating green fluorescent mice by germline transmission of green fluorescent ES cells. *Mech. Dev.* **76**, 79–90 (1998).
21. Tricoire, L. *et al.* A blueprint for the spatiotemporal origins of mouse hippocampal interneuron diversity. *J. Neurosci.* **31**, 10948–10970 (2011).
22. Vignoli, T. *et al.* Consequences of pilocarpine-induced status epilepticus in immunodeficient mice. *Brain Res.* **1450**, 125–137 (2012).
23. Racine, R.J. Modification of seizure activity by electrical stimulation. II. Motor seizure. *Electroencephalogr. Clin. Neurophysiol.* **32**, 281–294 (1972).
24. Babb, T.L., Kupfer, W.R., Pretorius, J.K., Crandall, P.H. & Levesque, M.F. Synaptic reorganization by mossy fibers in human epileptic fascia dentata. *Neuroscience* **42**, 351–363 (1991).
25. Palmiter, R.D., Cole, T.B., Quaife, C.J. & Findley, S.D. ZnT-3, a putative transporter of zinc into synaptic vesicles. *Proc. Natl. Acad. Sci. USA* **93**, 14934–14939 (1996).
26. Hermann, B., Seidenberg, M. & Jones, J. The neurobehavioural comorbidities of epilepsy: can a natural history be developed. *Lancet Neurol.* **7**, 151–160 (2008).
27. D'Hooge, R. & De Deyn, P.P. Applications of the Morris water maze in the study of learning and memory. *Brain Res. Brain Res. Rev.* **36**, 60–90 (2001).
28. Palop, J.J. *et al.* Neuronal depletion of calcium-dependent proteins in the dentate gyrus is tightly linked to Alzheimer's disease–related cognitive deficits. *Proc. Natl. Acad. Sci. USA* **100**, 9572–9577 (2003).
29. Verret, L. *et al.* Inhibitory interneuron deficit links altered network activity and cognitive dysfunction in Alzheimer model. *Cell* **149**, 708–721 (2012).
30. Hirsch, J.C. *et al.* Deficit of quantal release of GABA in experimental models of temporal lobe epilepsy. *Nat. Neurosci.* **2**, 499–500 (1999).
31. Cossart, R. *et al.* Dendritic but not somatic GABAergic inhibition is decreased in experimental epilepsy. *Nat. Neurosci.* **4**, 52–62 (2001).
32. Kobayashi, M. & Buckmaster, P.S. Reduced inhibition of dentate granule cells in a model of temporal lobe epilepsy. *J. Neurosci.* **23**, 2440–2452 (2003).
33. Zipancic, I., Calcagnotto, M.E., Piquer-Gil, M., Mello, L.E. & Alvarez-Dolado, M. Transplant of GABAergic precursors restores hippocampal inhibitory function in a mouse model of seizure susceptibility. *Cell Transplant.* **19**, 549–564 (2010).
34. Chagnac-Amitai, Y. & Connors, B.W. Horizontal spread of synchronized activity in neocortex and its control by GABA-mediated inhibition. *J. Neurophysiol.* **61**, 747–758 (1989).
35. Trevelyan, A.J., Sussillo, D. & Yuste, R.M. Feedforward inhibition contributes to the control of the speed of epileptiform propagation. *J. Neurosci.* **27**, 3383–3387 (2007).
36. Schevon, C.A. *et al.* Evidence of an inhibitory restraint of seizure activity in humans. *Nat. Commun.* **3**, 1060 (2012).
37. Berényi, A., Belluscio, M., Mao, D. & Buzsaki, G. Closed-loop control of epilepsy by transcranial electrical stimulation. *Science* **337**, 735–737 (2012).

ONLINE METHODS

Animals. Mice were maintained in standard housing conditions on a 12-h light/dark cycle with food and water provided *ad libitum*. All protocols and procedures followed the guidelines of the Laboratory Animal Resource Center at the University of California, San Francisco. The young adult CD1 mice used for pilocarpine injections and breeding were purchased from Charles River Laboratories. Embryonic donor tissue was produced by crossing wild-type CD1 mice to homozygous *GFP*$^+$ mice[20]. Pilocarpine injections (289 mg per kg of body weight) were performed in adult P51 male mice as described previously[15]. After recovering from acute status epilepticus, mice were housed singly and monitored for chronic spontaneous seizures between 9 and 20 d after pilocarpine administration by video recording. Mice only became candidates for transplantation after motor seizures of grade 3 or greater were detected, according to a modified Racine rating scale[15,23]. Mice that were not observed to have spontaneous seizures were killed around 25 d after pilocarpine injection.

Tissue dissection and transplantation. Ventricular and subventricular layers of the MGE were harvested from E13.5 *GFP*+ embryos. The time point at which the sperm plug was detected was considered E0.5. Embryonic MGE explants were dissected in Leibovitz L-15 medium, mechanically dissociated by repeated pipetting in medium containing DNase I (100 μg ml^{-1}) and concentrated by centrifugation (2 min at 1,000 *g*). Concentrated cell suspensions (~10^3 cells nl^{-1}) were front loaded into bevelled glass micropipettes (40–50-μm tip diameter, Wiretol 5 μl, Drummond Scientific) and injected (3×10^4 cells per injection) into the hippocampus or amygdala of adult control or epileptic CD1 mice (P60–76). All injection coordinates were first verified in a series of preliminary dye and/or cell injection studies into control and epileptic mice (**Supplementary Fig. 6**). For hippocampal transplantations, injections were made into stratum radiatum of the CA3 subfield at the following stereotaxic coordinates: anterior-posterior (AP) 1.75 mm, medial-lateral (ML) 2.3 mm, dorsal-ventral (DV) 1.7 mm. A second group of injections were made at three sites along the length of the hippocampus: AP 3.25 mm, ML 3.0 mm and DV 3.65 mm, 2.9 mm and 2.0 mm. For amygdala transplantations, injections were made into the basolateral nuclei at AP 1.5 mm, ML 3.65 mm and DV 3.7 mm. Sham-operated controls were injected with an equal volume of vehicle at each site (that is, four sites per hemisphere for hippocampus, one site per hemisphere for amygdala). For migration studies, only a single injection was made into the right, dorsal CA3 region of the hippocampus. For behavior and EEG experiments, transplantations were only considered to be successful if the density and migration of GFP cells in the recipient brain were evenly distributed in both hemispheres and confirmed as ≥30,000 cells (hippocampus, range = 34,200 to 68,100) or ≥5,000 cells (amygdala, range = 5,800 to 8,600) per mouse and ≥600 μm from the injection site; these criteria were met in all mice. Cell viability (74.1 ± 1.7%) and concentration were quantified using 0.5 μl of the cell suspension mixed with 24.5 μl of L-15 medium and 25 μl of Trypan Blue (Sigma) as described previously[38].

Immunostaining. Mice were transcardially perfused with 4% paraformaldehyde (vol/vol) and free-floating vibratome sections (50 μm) were processed using standard immunostaining procedures[12–14]. Primary antibodies and dilutions are provided in **Supplementary Table 4**. For ZnT3 staining, we used a TSA Cyanine 3 System kit (PerkinElmer, NEL704A001KT) for signal amplification. For secondary antibodies (1:500, Invitrogen), we used Alexa 488–conjugated goat antibody to chicken IgG (cat. #A11039) and Alexa 594–conjugated goat antibody to mouse IgG (cat. #A11005), goat antibody to rabbit IgG (cat. #A11012), goat antibody to guinea pig IgG (cat. #A11076) and donkey antibody to goat IgG (cat. #A11058). Sections were then mounted on charged slides (Superfrost plus, Fisher Scientific) with Vectashield that contained DAPI. Images were obtained with a spinning disk confocal microscope (Nikon Yokogawa CSU-X1 Borealis). Epifluorescent images were obtained using a Nikon Eclipse microscope. Brightness and contrast were adjusted manually using Adobe Photoshop.

Cell quantification. Transplanted GFP-labeled cells were directly counted in fluorescently labeled sections (50 μm) from recipient mice as described previously[12–14]. All transplanted cells that expressed GFP were counted in every sixth coronal section in all layers of the entire hippocampus or amygdala (that is, 300 μm apart) using a Nikon Eclipse microscope with a 40× objective.

Electrophysiology. Coronal brain slices (300 μm thickness) were prepared from recipient mice 60–65 DAT. Slices were submerged in the recording chamber and continuously perfused with oxygenated artificial cerebrospinal fluid (32–34 °C) containing 124 mM NaCl, 3 mM KCl, 1.25 mM NaH_2PO_4-H_2O, 2 mM $MgSO_4$-$7H_2O$, 26 mM $NaHCO_3$, 10 mM dextrose and 2 mM $CaCl_2$ (pH 7.2–7.4, 300–305 mOsm kg^{-1}). Whole-cell patch-clamp recordings from GFP-labeled cells were performed at 40× using an upright, fixed-stage microscope (Olympus BX50WI) equipped with infrared differential interference contrast and epifluorescence optics. Patch pipettes (3–5 MΩ) were filled with an internal solution containing 140 mM potassium gluconate, 1 mM NaCl, 5 mM EGTA, 10 mM HEPES, 1 mM $MgCl_2$, 1 mM $CaCl_2$, 3 mM KOH, 2 mM ATP and 0.2% biocytin (wt/vol), pH 7.21. Recordings were obtained with an Axopatch 1D amplifier, filtered at 5 kHz, and recorded to pClamp 10.2 software (Clampfit, Axon Instruments). Spontaneous EPSCs were examined at a holding potential of −70 mV. Series resistance was typically <15 MΩ and was monitored throughout the recordings. Data were only used for analysis if the series resistance remained <20 MΩ and changed by ≤20% during the recordings. Recordings were not corrected for a liquid junction potential. Resting membrane potentials were measured immediately after breakthrough by temporarily removing the voltage clamp and monitoring voltage. For current-clamp recordings, cells were held at −70 mV, and electrophysiological properties were measured in response to a series of long (1,000 ms) hyperpolarizing and depolarizing current-injections (10 pA steps, range = −80–1,000 pA). Data analysis was performed using pClamp 10.2 (Clampfit, Axon Instruments), MiniAnalysis 6.0 (Synaptosoft), Microsoft Excel and Sigmaplot 12.3 programs. A 2-min sample recording per cell was used for measuring EPSC characteristics. Events characterized by a typical fast rising phase and exponential decay phase were manually detected using MiniAnalysis. The threshold for event detection was currents with amplitudes greater than three times the root mean square noise level.

Single-cell RT-PCR. At the end of the recording session (<15 min), we aspirated the cytoplasm of the cell into the recording pipette while maintaining a tight seal, similar to methods described previously[21]. The pipette was carefully removed and its contents (~6 μl) were expelled into a test tube containing 1.5 μl of nuclease free water and 1 μl of RNaseOUT (40 U μl^{-1}) and stored at −80 °C. Samples were incubated with DNase I (Invitrogen) according to manufacturer instructions for complete removal of genomic DNA. Reverse transcription was then performed using 2 μl of 10× reverse transcription buffer, 1 μl of mixed 10mM deoxy NTPs, 4 μl of 25 mM $MgCl_2$, 2 μl of 0.1 M DTT, 1 μl of random hexamer (50 ng μl^{-1}) and 1 μl of SuperScript III reverse transcription (Invitrogen) in a final volume of 22 μl. Next, two consecutive rounds of PCR were performed using outer and nested primer pairs[21,39] (**Supplementary Table 1**). All targets were first amplified simultaneously using 1 μl of each primer (20 pmol μl^{-1}) and 40 μl of 2× GoTaq Green Master Mix in a final volume of 100 μl. Targets were amplified using 5 min of initial denaturation at 94 °C followed by 21 cycles of denaturing at 94 °C for 30 s, annealing at 60 °C for 30 s, elongation at 72 °C for 35 s and 7 min of final elongation at 72 °C. Next, individual targets were re-amplified separately for 20 cycles of PCR with the same thermal cycling conditions using 3 μl of the first PCR product as a template and nested primer sets. Products were assayed on a 1.5% agarose gel stained with ethidium bromide, using a 100-bp DNA ladder (Thermo Scientific) as a molecular weight marker. All primer sets were first verified on 1 ng of total RNA purified from GFP mouse hippocampus using the RT-PCR protocol described above ($n = 2$ samples; **Fig. 2f** and **Supplementary Table 1**). To rule out mRNA contamination from surrounding tissue, we placed patch pipettes into the slice without seal formation and, after the removal of the pipette, processed its content as described above ($n = 3$ samples). To rule out contamination of reaction materials, PCR was performed using nuclease-free water in place of a sample ($n = 5$ samples). No PCR product was obtained using these protocols.

Video-EEG. EEG recordings were obtained using a time-locked video-EEG monitoring system (Pinnacle Technologies). Each mouse was anesthetized with ketamine and xylazine (10 and 1 mg per kg, intraperitoneal) so that there was no limb-withdrawal response to a noxious foot pinch. Sterile, stainless steel bone screw recording electrodes were placed epidurally through burr holes in the skull (one electrode on either side of the sagittal suture, approximately halfway between bregman and lambdoid sutures and ≈1 mm from the midline) using surface head-mount EEG hardware (Pinnacle Technologies). Electrodes were cemented

doi:10.1038/nn.3392

in place with a fast-acting adhesive and dental acrylic. Two wires were laid on the shoulder muscles for electromyographic recording. Mice were allowed to recover for 3 d before experiments were initiated. Electrographic seizures were defined as high-frequency, high-voltage synchronized polyspike or paroxysmal sharp waves with amplitude more than twofold greater than background that lasted ≥15 s. Electrographic EEG seizures were analyzed by two investigators who were blinded to the treatment condition of the mice using SireniaScore software (Pinnacle) and confirmed by offline review of behavioral video recordings obtained at two different viewing angles. Behaviors were scored according to a modified Racine rating scale[12,23]. Experimental mice were monitored for 7–10 d (24 h d^{-1}). Because electrographic seizure characteristics in untreated and vehicle-injected epileptic mice were comparable in frequency (2.8 ± 0.5 versus 1.9 ± 0.4 seizures per d, $P = 0.3$, two-tailed t test) and duration (54.4 ± 2.8 versus 56.0 ± 3.1 s, $P = 0.8$, two-tailed t test), the data from these groups were pooled. A total of 24 d of recording were analyzed for control mice ($n = 3$), 111 d for untreated or vehicle-treated epileptic mice ($n = 14$), 64 d for mice that received MGE cell grafts into the hippocampus ($n = 8$) and 65 d for mice that received MGE cell grafts into the amygdala ($n = 8$).

Behavior. All behavioral testing was conducted during the light phase of the light/dark cycle under the guidance and supervision of the University of California at San Francisco Neurobehavioral Core for Rehabilitation Research facility. Pilocarpine-injected mice and age-matched controls were housed singly starting immediately after the induction of status epilepticus. Mice were tested in two separate groups. Group 1 was subjected to the open field test (before pilocarpine injections), open field test (14 d after pilocarpine injections), handling test around 60 DAT, open field test ~24 h after the handling test, rotarod immediately following the final open field session and then 2–3 d later, and EEG surgery and monitoring. Group 2 (60 DAT) was subjected to the elevated plus maze, Morris water maze and forced swim test. Mouse identities were coded, and all behaviors were performed and analyzed by two investigators who were blinded to the treatment condition of the animals.

Open field test. Mice were placed in the center of a 40 × 40 × 38 cm SmartFrame open field arena (Kinder Scientific) for 10 min under standard overhead lighting conditions. Behavioral performance was recorded using a computer-operated tracking system (MotorMonitor, Kinder Scientific).

Rotarod. Mice were placed on a rotarod apparatus (UGO-Basile, model 7650) that accelerated from 4 to 40 r.p.m. over 3.5 min and then maintained 40 r.p.m. for another 1.5 min. All mice were first acclimated to the rotarod immediately following the final open field testing session and then tested 2–3 d later. Performance was assessed by measuring the latency until the mouse fell completely off the rod or gripped the device and spun around without attempting to walk on the rod. Three trials were performed and both the r.p.m. reached and total time spent on the rod were averaged across the trials for each mouse.

Handling test. Reaction to handling was assessed using a semiquantitative handling test described previously[40]. The test included four measures: nonstressful handling was performed by rubbing slowly along the back of the mouse in a petting motion in the direction of the grain of fur with a latex-gloved hand, and stressful handling was performed by rubbing vigorously against the grain of fur, pinching at the tail tip with a plastic-tipped hemostat and pinching at the tail base. Each task was performed for 15 s. Reaction to handling was scored for each task using a four-point rating scale in which 1 indicated initial struggle, but calmed within 15 s, 2 indicated struggle for more than 15 s, 3 indicated struggle for more than 15 s and exhibiting one or more defensive reactions (piloerection, flattening of the ears against the head, attempt to bite or back away from the experimenter), and 4 indicated struggled for more than 15 s and exhibited flight behavior (loud vocalization or wild running).

Elevated plus maze. The elevated plus maze apparatus (Kinder Scientific) was comprised of two open arms (38 × 2 cm) and two enclosed arms (38 × 2 × 15 cm), elevated 64 cm above the floor level. Mice were placed in the central platform always facing the same open arm. Test duration was 10 min under standard overhead lighting conditions. All data were collected using Ethovision software (Noldus Information Technology).

Morris water maze. The Morris water maze task was conducted similar to the method described previously[28,41]. A white, circular pool (140 cm in diameter) was filled with water (22–24 °C) that was mixed with black, nontoxic paint to make it opaque, and a circular platform (15 cm in diameter) was submerged 1 cm beneath the surface of the water. The testing room was filled with a number of visual cues. Mice were first trained to locate a visible platform (days 1 and 2) and then a submerged hidden platform (days 3–5) in two daily sessions ~3.5 h apart. Each session consisted of three 60-s trials with an intertrial interval of 10–15 min. Mice were allowed to swim until they found the platform and, if they did not find the platform within 60 s, they were guided to it by the experimenter. During visible platform training, the platform was moved to a new, random location quadrant for each session, and mice were placed in a different starting location for each trial. Exclusion criteria for visible platform performance were defined as an average latency (mean of all trials in sessions 3 and 4) greater than the average escape latency plus two s.d. in naive controls[28]. During the hidden platform task, mice were placed in a different starting location for each trial, but the platform remained in the same location for each trial (in the center of the target quadrant). Time to reach the platform, path length and swim speed were recorded with a video tracking system (Noldus Information Technology). Because there were no substantial differences in average swim speeds between the treatment groups during the visible platform sessions (data not shown), the time required to locate the platform (escape latency) was used as the main measure for analysis. A probe trial was conducted 1 h after the final hidden platform testing session; the platform was removed, and mice were placed in the pool and allowed to swim for 60 s.

Forced swim test. The mouse forced swim test was conducted similar to the method described previously[42]. Mice were placed individually into glass cylinders (height = 40 cm, diameter = 15 cm) containing 22 cm of water (22–23 °C) for 6 min. The total duration of immobility was recorded during the last 4 min of the 6-min testing period. A mouse was considered to be immobile when it floated in an upright position and made only minimal movements to keep its head above water. Trials were video recorded and scored offline by an investigator blinded to the experimental outcome of each animal.

Statistical analysis. All analyses were performed with SigmaPlot 12.3 software and assessed for normality (Shapiro-Wilk) and variance. Data were compared by t test, one-way ANOVA for multiple comparisons, nonparametric one-way ANOVA on ranks or by two-way repeated-measures ANOVA. A Tukey's *post hoc* test was performed when appropriate. Sample sizes for behaviors significantly affected by MGE treatment were determined based on power analysis, as indicated in **Supplementary Table 3**. Data are expressed as mean ± s.e. and significance was set at $P < 0.05$.

38. Marchenko, S. & Flanagan, L. Counting human neural stem cells. *J. Vis. Exp.* **7**, 262 (2007).
39. Vucurovic, K. *et al*. Serotonin 3A receptor subtype as an early and protracted marker of cortical interneuron subpopulations. *Cereb. Cortex* **20**, 2333–2347 (2010).
40. Mortazavi, F., Ericson, M., Story, D., Hulce, V.D. & Dunbar, G.L. Spatial learning deficits and emotional impairments in pentylenetetrazole-kindled rats. *Epilepsy Behav.* **7**, 629–638 (2005).
41. Raber, J., Bongers, G., LeFevour, A., Buttini, M. & Mucke, L. Androgens protect against apilipoprotein E4-induced cognitive deficits. *J. Neurosci.* **22**, 5204–5209 (2002).
42. Can, A. *et al*. The mouse forced swim test. *J. Vis. Exp.* **59**, 3638 (2012).